Supporting Information for

ORIGINAL ARTICLE

A combined nanotherapeutic approach targeting farnesoid x receptor, ferroptosis, and fibrosis for nonalcoholic steatohepatitis treatment

Jiangtao Fu[a,†], Pingping Zhang[a,†], Zhiguo Sun[a,†], Guodong Lu[a,†], Qi Cao[a], Yiting Chen[a], Wenbin Wu[a], Jiabao Zhang[a,b], Chunlin Zhuang[a,b], Chunquan Sheng[a,b], Jiajun Xu[c*], Ying Lu[a,b*], Pei Wang[a,b*]

[a]*The Center for Basic Research and Innovation of Medicine and Pharmacy* (*MOE*), *School of Pharmacy, Naval Medical University, Shanghai 200433, China*

[b]*National Demonstration Center for Experimental Pharmaceutical Education, Naval Medical University/Second Military Medical University, Shanghai 200433, China*

[c]*Department of Diving and Hyperbaric Medicine, Naval Special Medical Center, Naval Medical University, Shanghai 200433, China*

Received 21 November 2023; received in revised form 26 December 2023; accepted 30 December 2023

[*]Correspondence authors.

E-mail addresses: pwang@smmu.edu.cn (Pei Wang), acuace@163.com (Ying Lu), xujiajun920@163.com (Jia-Jun Xu).

[†]These authors made equal contributions to this work.

Figure S1

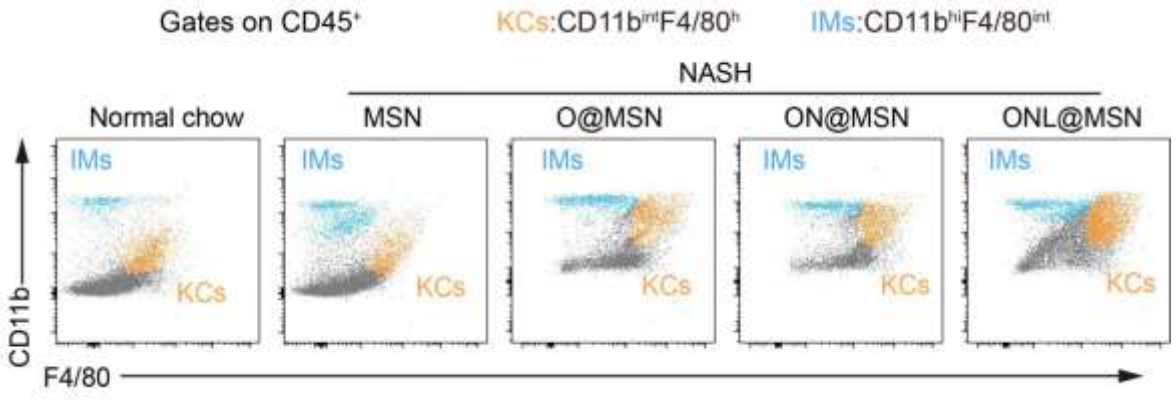

Representative flow cytometry analysis of Kupffer cells (KCs) and infiltrating monocytes (IMs) based on F4/80 and CD11b staining in $CD45^+$ leukocytes isolated from liver tissues. In the manual gating analysis, the $F4/80^{high}CD11b^{int}CD45^+$ cells were considered as KCs, whereas the $F4/80^{int}CD11b^{high}CD45^+$ cells were considered as IMs.

Figure S2

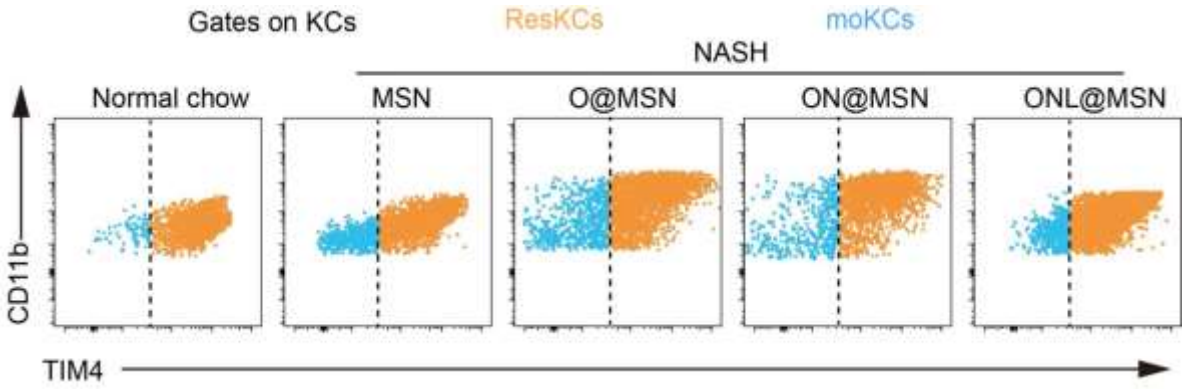

Representative flow cytometry analysis of yolk sac-derived resident KCs (ResKCs) and monocyte-derived KCs (MoKCs) based on TIM4 staining in KCs. In the manual gating analysis, the $TIM4^{high}F4/80^{high}CD11b^{int}CD45^{+}$ cells were considered as ResKCs, whereas the $TIM4^{low}F4/80^{high}CD11b^{int}CD45^{+}$ cells were considered as MoKCs. The former resolves inflammation whereas the later induces inflammation.

Figure S3

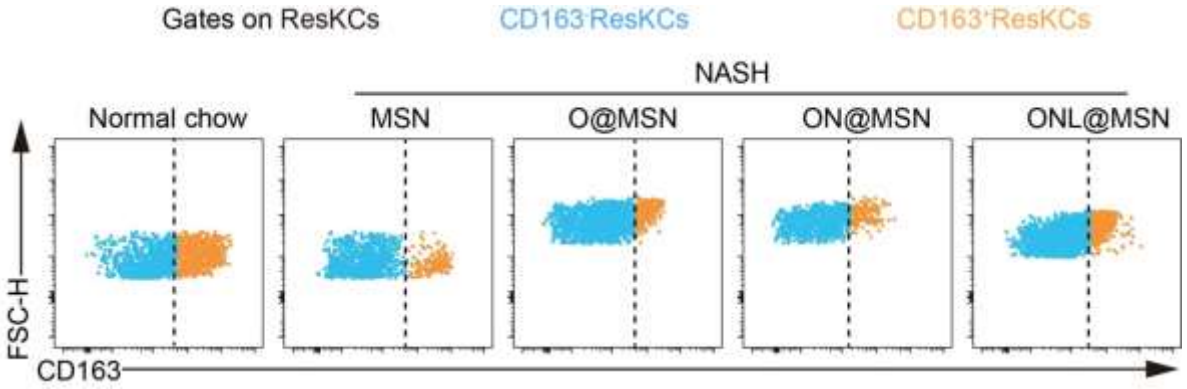

Representative flow cytometry analysis of $CD163^+$ ResKCs and $CD163^-$ ResKCs based on CD163 staining in ResKCs. CD163 is a member of the scavenger receptor cysteine-rich family and is expressed by anti-inflammatory M2 macrophages, which produce anti-inflammatory cytokines.

Figure S4

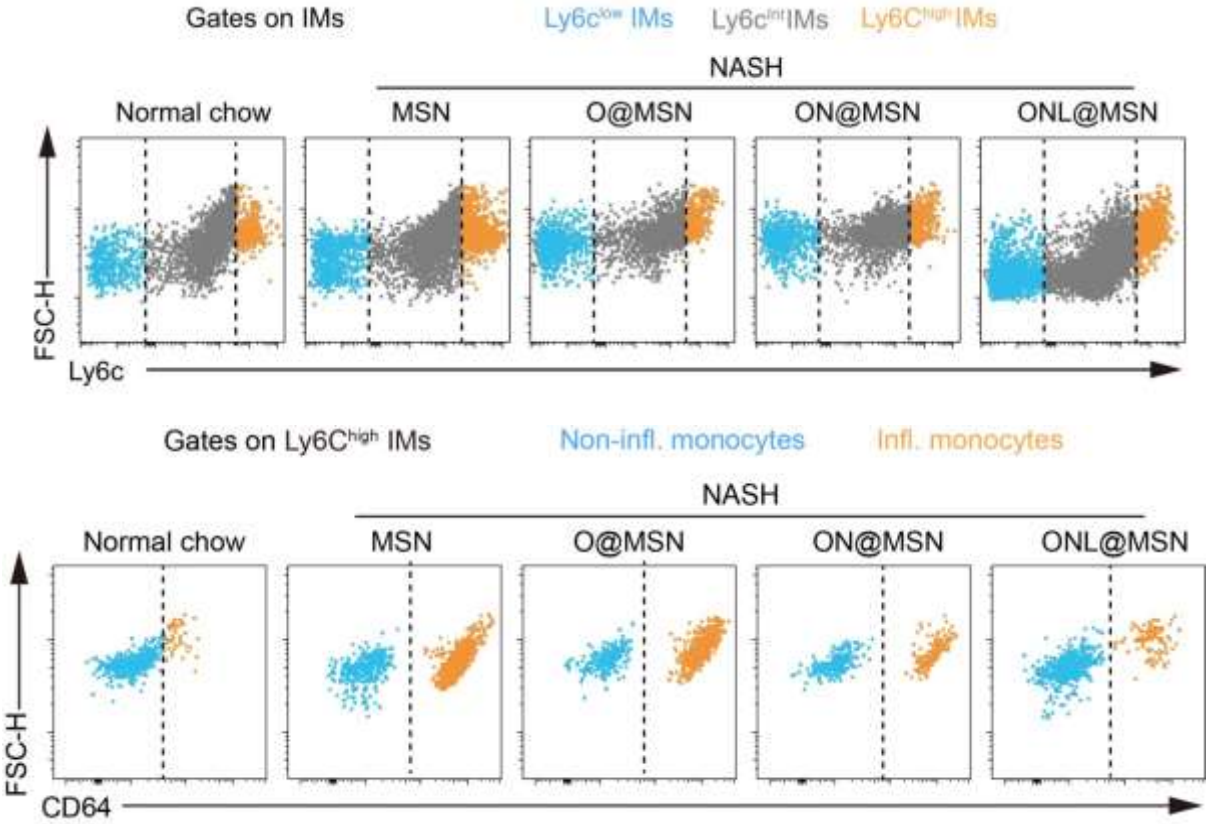

Representative flow cytometry analysis of Ly6C^{high} IMs, Ly6C^{Int} IMs and Ly6C^{low} IMs based on Ly6C staining in IMs (F4/80^{int}CD11b^{high}CD45^{+}), and the further clustering inflammatory monocytes (CD64^{+}Ly6C^{high} IMs) and non-inflammatory monocytes (CD64^{-}Ly6C^{high} IMs) based on CD64 staining in Ly6C^{high} IMs.

Figure S5

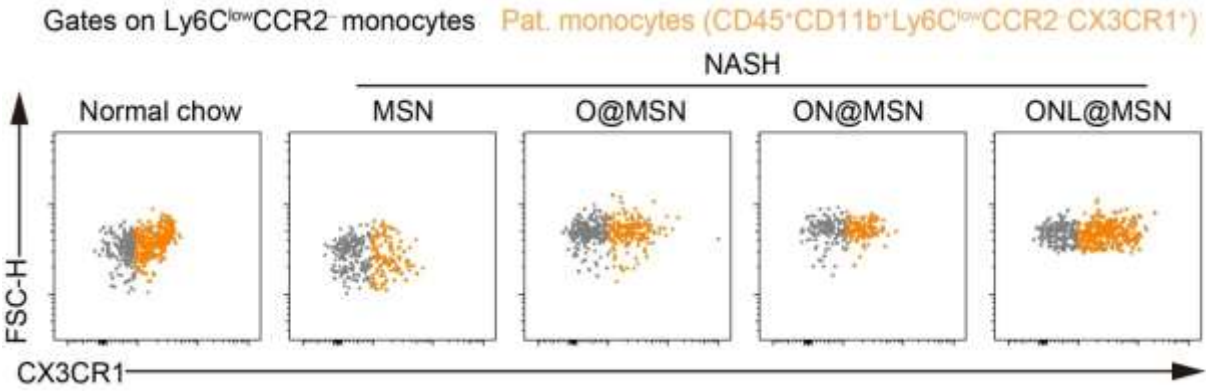

Representative flow cytometry analysis of patrolling monocytes ($CD45^{+}CD11b^{+}Ly6C^{low}CCR2^{-}CX3CR1^{+}$) based on CX3CR1 staining in $CD45^{+}CD11b^{+}Ly6C^{low}CCR2^{-}$ cells. In the manual gating analysis, the $CD45^{+}CD11b^{+}Ly6C^{low}CCR2^{-}CX3CR1^{+}$ monocytes are considered to be the patrolling monocytes.

Figure S6

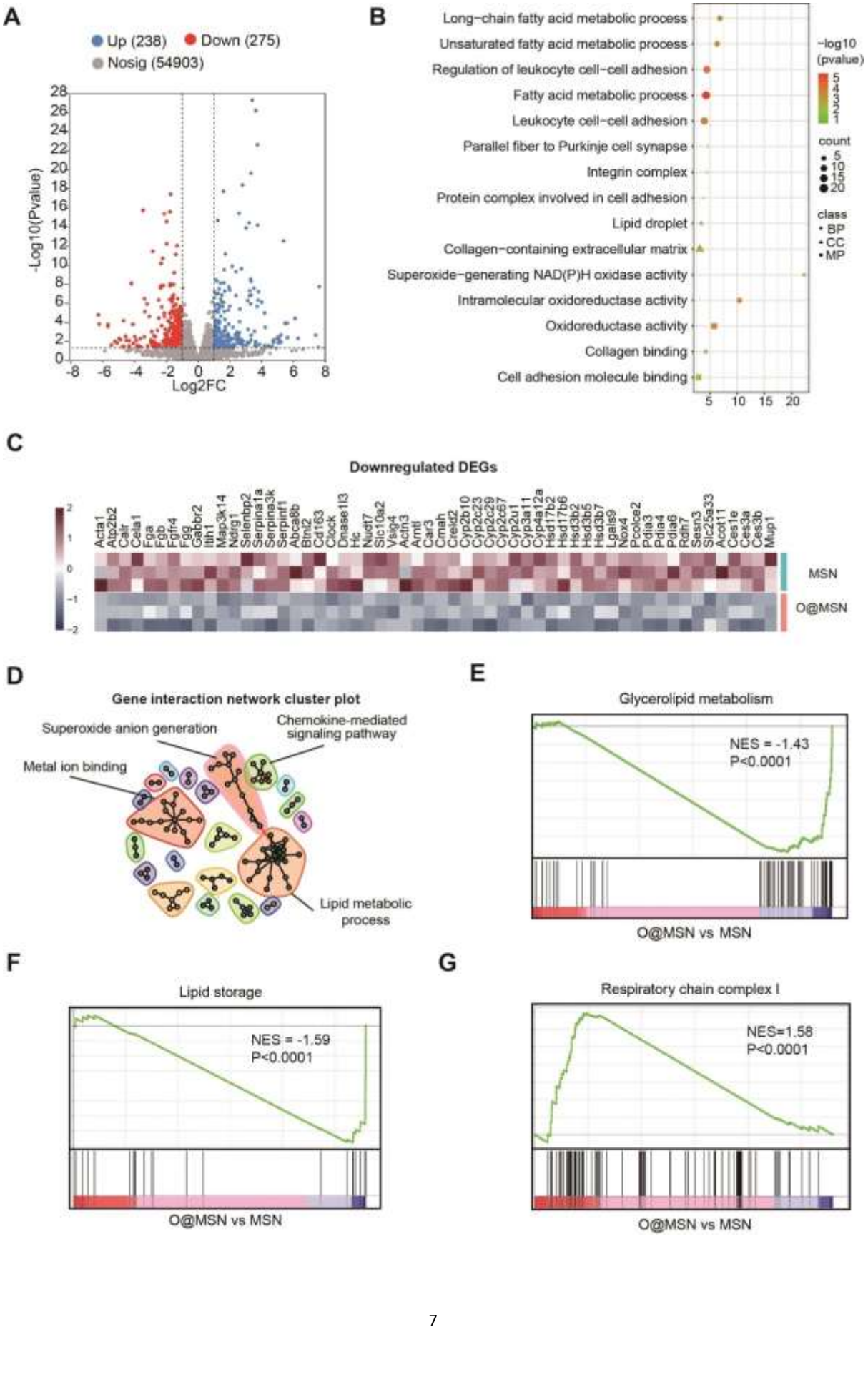
A
Up (238)
Down (275)
Nosig (54903)
-Log10(Pvalue)
Log2FC
B
Long−chain fatty acid metabolic process
Unsaturated fatty acid metabolic process
Regulation of leukocyte cell−cell adhesion
Fatty acid metabolic process
Leukocyte cell−cell adhesion
Parallel fiber to Purkinje cell synapse
Integrin complex
Protein complex involved in cell adhesion
Lipid droplet
Collagen−containing extracellular matrix
Superoxide−generating NAD(P)H oxidase activity
Intramolecular oxidoreductase activity
Oxidoreductase activity
Collagen binding
Cell adhesion molecule binding
−log10 (pvalue)
count
class
BP
CC
MP
C
Downregulated DEGs
MSN
O@MSN
D
Gene interaction network cluster plot
Superoxide anion generation
Chemokine-mediated signaling pathway
Metal ion binding
Lipid metabolic process
E
Glycerolipid metabolism
NES = -1.43
P<0.0001
O@MSN vs MSN
F
Lipid storage
NES = -1.59
P<0.0001
O@MSN vs MSN
G
Respiratory chain complex I
NES=1.58
P<0.0001
O@MSN vs MSN

Bulk-tissue RNA sequencing shows the effects of O@MSN on transcriptome in liver tissue of NASH mice.

(A) Volcano plot showing the upregulated DEGs (n = 163) and downregulated DEGs (n = 199) in liver tissue of mice by treatment of O@MSN compared with MSN.

(B) KEGG plot showing the mainly processes altered by O@MSN compared with MSN in molecular function (MF), biological process (BP) and cell component (CC).

(C) Heatmap plot showing the Top DEGs modulated by O@MSN.

(D) Gene interaction network cluster plot showing the major important modules interacting with other genes altered by treatment of O@MSN compared with MSN.

(E-G) Gene Set Enrichment Analysis (GSEA) plot showing several enriched signaling pathways by treatment of O@MSN compared with MSN.

Figure S7

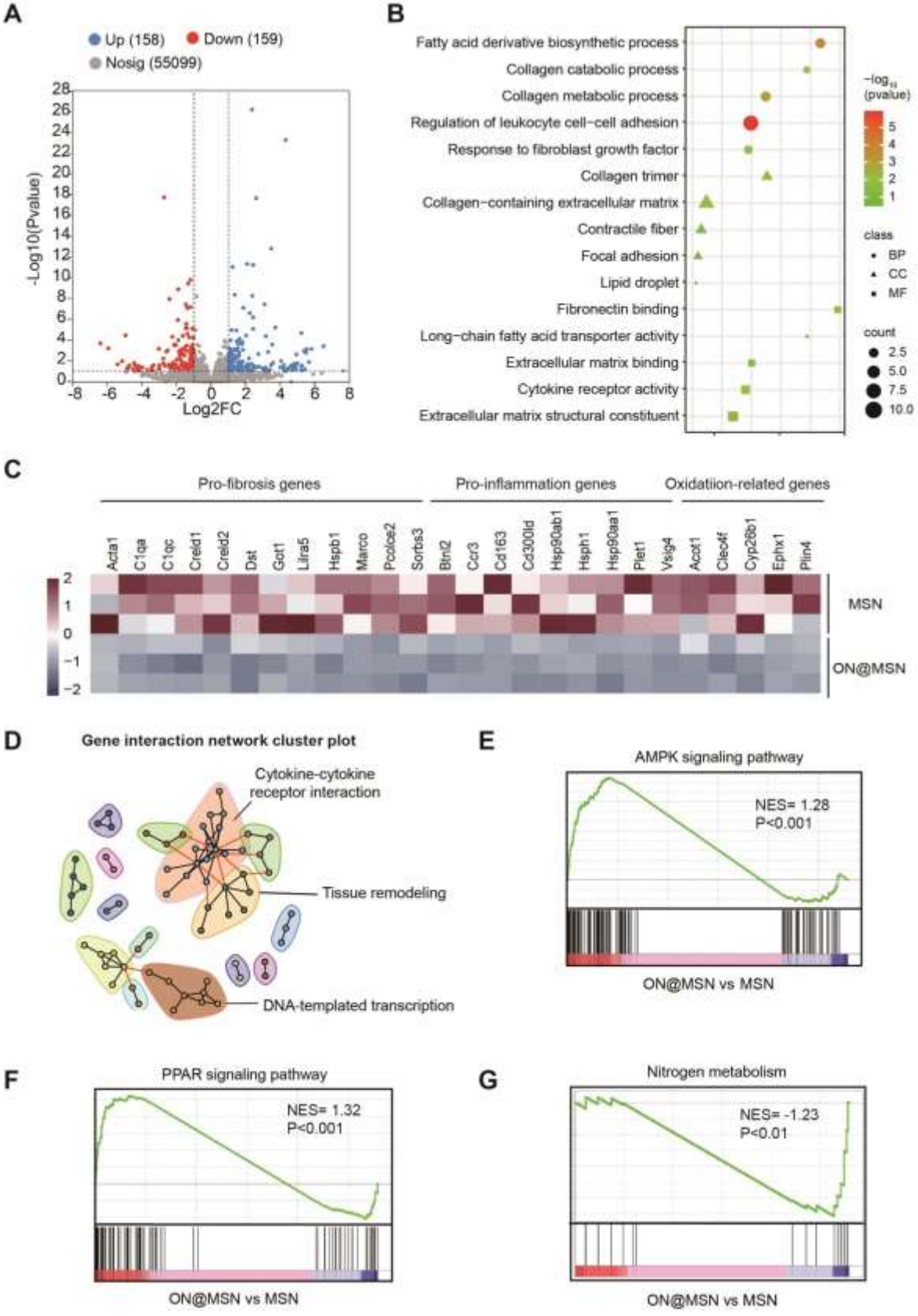

Bulk-tissue RNA sequencing shows the effects of ONL@MSN on transcriptome in liver tissue of NASH mice.

(A) The experimental design of bulk-tissue RNA sequencing on liver tissues of mice receiving treatment of ONL@MSN or MSN (control).

(B) Correlation between the samples from two groups.

(C) Volcano plot showing the upregulated DEGs (n = 163) and downregulated DEGs (n = 199) in liver tissue of mice receiving treatment of ONL@MSN compared with that of mice receiving treatment of MSN.

Figure S8

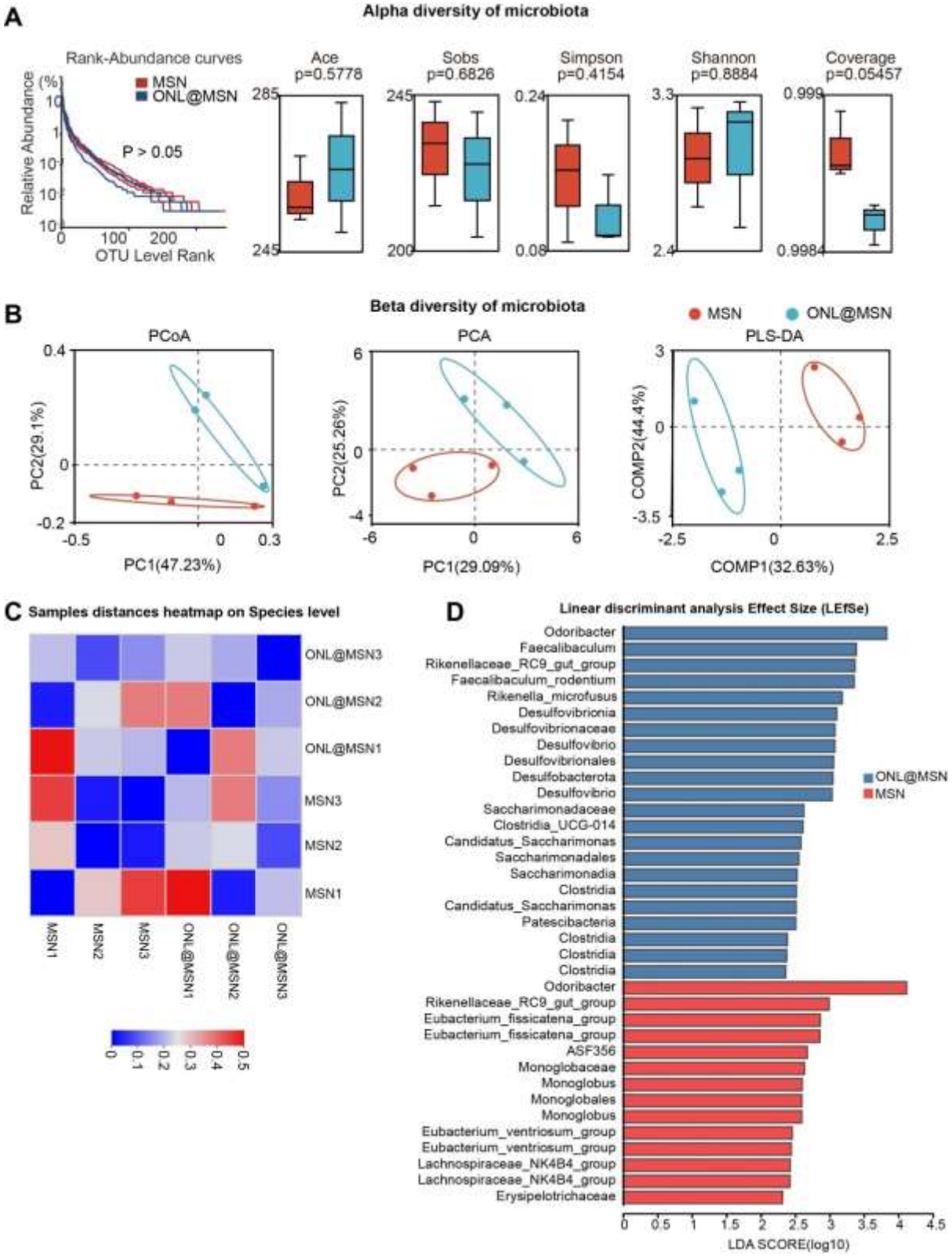

Fecal 16S-rRNA sequencing shows the effects of ONL@MSN on gut microbiota community in NASH mice.

(A) The Alpha diversity of gut microbiota in feces of mice receiving treatment of ONL@MSN or MSN (control).

(B) The Beta diversity of gut microbiota in feces of mice receiving treatment of ONL@MSN or MSN (control).

(C) Correlation between the gut microbiota community in samples from two groups.

(D) LEfSe of gut microbiota community in samples from two group.

Table S1 Drug loading efficiency of nanoparticles.

Nanoparticle	Drug loading efficiency (%)	Entrapment efficiency (%)
O@MSN (OCA)	67.70 ± 0.22	66.03±0.21
ON@MSN (OCA)	61.55 ± 0.12	59.75±0.12
ONL@MSN (OCA)	54.21 ± 0.06	53.03±0.06
ONL@MSN (Liproxsatin-1)	50.17 ± 0.12	49.91±0.12

Data are expressed as mean ± SD (n = 3).

Table S2 Primers for real-time PCR.

Gene	Forward	Reverse
Cxcl1	CACCCAAACCGAAGTCATAGC	GGGGACACCTTTTAGCATCTTT
Ccl2	TGAGGTGGTTGTGGAAAAGG	CCGTAGCGTTGGGTTTCT
Ccl5	ACTCCCTGCTGCTTTGCC	CTGGTGTAGAAATACTCCTTGACG
Tnf-α	TTCTCATTCCTGCTTGTGG	CACTTGGTGGTTTGCTACG
Il-1β	CAGGCTCCGAGATGAAC	TGCTTGTGAGGTGCTGA
Il-6	TGGGACTGATGCTGGTG	CTGGCTTTGTCTTTCTTGTTA
Gapdh	CCCATCACCATCTTCCAG	ATGGGGAAGGTGAAGGTCG